ISSN 0208-7774 TRIBOLOGIA 3/2020 p. 53–62
DOI: 10.5604/01.3001.0014.4765

Mariusz WARZECHA*

A MATHEMATICAL MODEL AND A SIMULATIONAL INVESTIGATION OF A PLANAR SYSTEM UNDER OBLIQUE MULTIPOINT IMPACT WITH FRICTION

MODEL I BADANIA SYMULACYJNE ZDERZENIA WIELOPUNKTOWEGO W PŁASKIM UKŁADZIE WIELOCZŁONOWYM Z UWZGLĘDNIENIEM TARCIA

Key words: multibody system, contact, energy dissipation, stick-slip, collision, compliance model, coefficient of restitution.

Abstract: This article presents a mathematical model of a planar system for the multipoint, oblique, and eccentric impact of rough bodies. The created model served for numerical investigations of the system's behaviour. To analyse the influence of various parameters, three simplified cases were defined. Each of these cases focused on different aspects of the simulation. The first case was used to determine how many contacting bodies undergo impact at a given time point. This result was then compared with the experimental observations, which gave good agreement. The second case investigated the influence of the body configuration and the coefficient of friction (COF) on the sliding process during impact. Depending on the parameter values, the sliding process was divided into three main areas: slip-reversal slip, stick-slip, and continuous slip with increasing sliding velocity. The third case focused on the energy dissipation expressed by the coefficient of restitution (COR) and the angle of incidence of the initiating impact; this case showed possible improvement areas of the used impact force model.

Słowa kluczowe: dyssypacja energii, kontakt, zderzenia ukośne, stick-slip, model podatny, współczynnik restytucji.

Streszczenie: W artykule przedstawiono model matematyczny płaskiego zderzenia wielopunktowego. Konfiguracja zderzających się ciał pozwalała na wystąpienie zarówno zderzenia mimośrodowego jak i ukośnego oraz uwzględniała tarcie. Opracowany model posłużył następnie badaniom symulacyjnym. W celu przeanalizowania wpływu różnych parametrów na zachowanie systemu zdefiniowano trzy uproszczone przypadki. W pierwszym badano, jaka ilość ciał bierze jednocześnie udział w zderzeniu. Przeprowadzone porównanie otrzymanych wyników z obserwacjami eksperymentu pokazało dobrą zgodność. W drugim przypadku badano wpływ konfiguracji zderzających się ciał oraz współczynnika tarcia na przebieg procesu poślizgu w trakcie zderzenia. W zależności od wartości parametrów możliwe są trzy główne scenariusze: poślizg–zmiana kierunku poślizgu, poślizg–zatrzymanie poślizgu, ciągły poślizg ze wzrastającą prędkością poślizgu. Trzeci przypadek skupiał się na dyssypacji energii wyrażonej poprzez współczynnik restytucji oraz kierunku uderzenia inicjującego; przypadek ten pokazał obszary, w których wykorzystany model siły zderzenia wymaga dopracowania.

INTRODUCTION

An impact phenomenon occurs commonly during the work of technical systems. Defined as an event occurring during contact between bodies moving with a negative normal component of relative velocity, it exists during the work of, e.g., inertial grids, vibratory transport systems, hammer crushers, cars, or robots **[L. 1–3]**. Therefore, a better understanding of the impact phenomenon and, in consequence, an improved ability to model it is of vital importance for mechanical engineers.

The effects of friction can significantly complicate the modelling and analysis of impact. During impact, the friction force may not be unidirectional or continuous

* ORCID: 0000-0002-7417-1561, AGH University of Science and Technology, Faculty of Mechanical Engineering and Robotics, Mickiewicza 30 Ave., 30-059 Kraków, Poland, e-mail: mwarzech@agh.edu.pl.

and can bring the initial slip to rest before the end of the impact or cause a reversal of sliding velocity. Nevertheless, various studies have included friction in the impact analysis of two rigid bodies **[L. 4–7]**. Those studies are based mainly on assumptions that impacting bodies are non-slender (energy loss due to elastic waves is small) and hard enough to keep the contact area very small in correspondence to body dimensions.

Routh's method applied to the analysis of two-dimensional impact with friction allowed the classification of possible cases by the locations of the line of sticking and the line of maximum compression **[L. 6]**. The mentioned article also indicated a difference in the obtained results when applying Newton's and Poisson's definitions of the coefficient of restitution (COR). A more recent study **[L.** 7**]** applied an energetic definition of COR. It used the impulse of normal collision force as an independent variable and divided the behaviour of impacting bodies resulting from friction into continuous slip, slip-stick, slip-reverse slip, and jam-stick. This behaviour can be predicted for particular impacting bodies and is dependent on the value of the coefficient of friction (COF) and the parameter describing their configuration (level of eccentricity).

To apply analogous methods for analysis of multipoint impact in a multibody system, an additional assumption is necessary. Namely, it should be assumed that all impacts occur at the same time (simultaneous approach) or that they take place one after another (sequential approach). The applications of both approaches can be found in the literature **[L. 8–11],** but it has been shown **[L. 12, 13]** that both of them can be used only in a limited number of cases and, in general, give results that do not agree with experiments and common sense.

An alternative approach to the rigid body solution is based on the assumption that impacting bodies are compliant in the vicinity of their contact point. Such an assumption allows an expression of the impact force as a function of body deformations. Therefore, this approach requires a model which expresses impact force in the local deformations of impacting bodies. Many models have been developed over the years. Most of them are based on the Hertz contact law. An overview of such models was presented in **[L. 14–16]**. Those models have been applied to the analysis of an impact of two bodies **[L. 17–21]**, although only a few of the published research studies includes friction **[L. 22, 23]**. All the research referenced above used the Coulomb-Antonow model of friction.

There are no additional assumptions required to apply the compliance method to multipoint impact. Stronge **[L. 24]** analysed the central impact of a system consisting of up to six balls. This study assumed perfectly elastic impacts and neglected friction. Similar assumptions were made in **[L. 11]**. In another work **[L. 12]**, the approach was extended to include energy dissipation expressed by the COR, but still there is no research investigating the multipoint collision of compliant, rough bodies, where friction cannot be neglected.

This article develops a model of the multipoint, oblique, and eccentric impact of rough bodies. To accomplish this task, a set of differential equations describing the system was written and is presented in the following section. Those equations were implemented in the Python script and used for numerical investigation of the system behaviour under various initial conditions for changing values of COR and COF. The effects of those investigations are shown in the results and discussion section, which is then followed by the summary.

The posed problem involves several questions. What impact force model is most suitable for multipoint impact modelling? Is this model satisfactory or is there a need for further development? Do the numerical implementations offer solutions in a given parameter range? How expensive computationally is the solution? The answers to these questions are discussed through the following sections and summarized in the conclusions.

METHODOLOGY

The system analysed in this article consisted of 3 up to 6 bodies. The limitation to 6 bodies can be justified by an experimental study **[L. 25]**. It investigated a linear pattern of thin discs and showed that a solitary strain/stress wave length generated by a small explosive charge was equal roughly to triple the disc diameter. This means that, at a particular time point, three discs were undergoing deformation. Therefore, it seems reasonable that analysis of the chain of 6 bodies should allow proper consideration of the occurring physical phenomena.

The bodies in the modelled system had the masses $M_1, M_2 \ldots M_j$ and inertia moments about their mass centres $J_1, J_2 \ldots J_j, j = 1 \ldots 6$. All of these bodies had a regular shape in the vicinity of the contact point O_i, $i = 1 \ldots 5$, as shown in **Fig. 1**, which allowed the creation of common tangent planes at all impact points. **Figure 1** also presents global and local coordinate systems. Each body has a local coordinate system $C_j x_j y_j$ at its mass centre. Additionally, each impact point O_i has a coordinate system defined in such a way that one axis is collinear with impact normal and the second is laid in a common tangent plane. Each of these coordinate systems is identified by subscript numbers, as evident from **Fig. 1**.

Several assumptions were made during the modelling process. They were as follows:

- Surfaces of contacting bodies are rough (friction cannot be neglected).
- All bodies are regular in the vicinity of the contact point and their surfaces in this area can be represented by sphere fragments.

– All bodies move in a planar motion; both eccentric and oblique impacts are possible.
– The impact force model expresses energy lost by the COR.

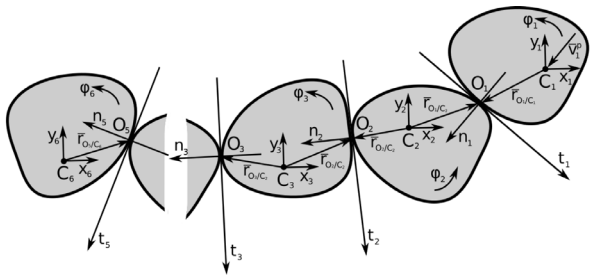

Fig. 1. Analysed system of bodies with defined coordinate systems

Rys. 1. Analizowany układ ciał wraz ze zdefiniowanymi układami współrzędnych

Contact force models

The impacting bodies deform each other in the vicinity of the contact point. Such deformation results in a contact force, which prohibits penetration of the bodies. Many contact force models have been developed over the years **[L. 14, 26]** and adapted for impact modelling. In general, those models can be divided into three groups: (1) pure elastic models, for example **[L. 27, 28]**; (2) models expressing energy dissipation in terms of plastic deformation, for example **[L. 29–31]**; and, (3) models using the coefficient of restitution to express energy dissipation, for example **[L. 32–38]**. Although they differently express energy dissipation, the majority of these models are based on the contact law proposed by Hertz **[L. 27]**.

A review of the available contact force models leads to the conclusion that, in the context of the proposed assumptions, the models from the third group are the most suitable. Although models in this group express energy dissipation during impact in terms of COR, they differ in its mathematical implementation. The model proposed by Hunt and Crossley **[L. 33]** and its later modifications **[L. 35–37]** extended the purely elastic Hertz model with the addition of a damping force. Such a damping force is proportional to the relative velocity of the impacting bodies. Hence, it results in the highest values of energy dissipation at the beginning and end of the impact. Such behaviour contradicts experimental results and common sense. Therefore, to avoid it, the damping force is multiplied by the bodies' indentation, which is 0 at the beginning and end of the impact. The damping force introduces the energy dissipation to the model. The amount of the energy dissipated during impact depends on the hysteresis damping factor. This factor is generally difficult to obtain, as it incorporates various sources of energy loss. Nevertheless, it can be expressed by the COR, which is a common way of expressing energy dissipation in impact modelling. Various relations for the hysteresis damping factor have been proposed, resulting in different impact force models. **[L. 14]** Equation (1) presents an example of the impact force model expressing the energy dissipation by the damping force, which was proposed by Flores et al. **[L. 37]**.

Another way of expressing the energy dissipation in terms of COR was used in the impact force model proposed by Michalczyk **[L. 32]**. This model assumes that the compression phase of the impact is fully elastic and introduces the energy dissipation at the beginning of the restitution phase by altering the contact stiffness. Such an approach was justified by the change in the physical properties of impacting bodies in the vicinity of the contact point, but it is rather a general statement and can include other phenomena such as the plastic deformation of the impacting bodies. The impact force resulting from this model was given by Eq. 2.

$$F_F = k\xi^n\left(1+\frac{8(1-R)}{5R}\frac{\dot{\xi}}{\dot{\xi}^0}\right) \tag{1}$$

$$F_M = k\xi^n\left(1-\frac{1-R^2}{2}\left\{1-sgn\left(\dot{\xi}\right)\right\}\right) \tag{2}$$

where R is the coefficient of restitution, k is the contact stiffness, ξ is the bodies' indentation and $\dot{\xi}$, are $\dot{\xi}^0$, respectively, impact velocity and its initial value.

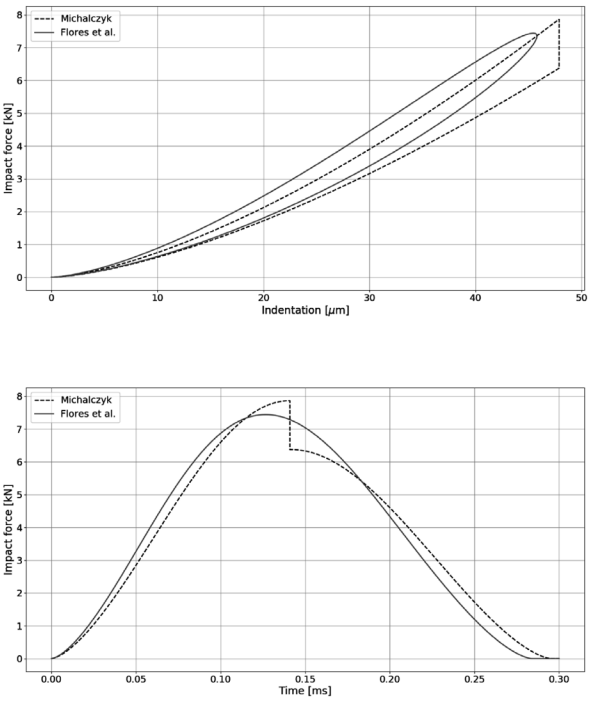

Fig. 2. Comparison of force models proposed by Michalczyk [L. 32] and Flores et al. [L. 37]

Rys. 2. Porównanie modeli siły zderzenia zaproponowanych przez Michalczyk **[L. 32]** oraz Flores et al. **[L. 37]**

The models proposed by Michalczyk **[L. 32]** and Flores et al. **[L. 37]** were chosen for direct comparison, because both equate the internal damping energy loss to the loss of kinetic energy in order to determine coefficients needed for the impact force model. Additionally, both models are suitable for use in a wide range of COR values. The impact forces resulting from these models are plotted in **Fig. 2**. An inspection of this figure indicates that the main difference between both impact force models is related to continuity. The model proposed by Flores et al. results in a continuous impact force, whereas the model developed by Michalczyk is discontinuous. The continuity of the Flores et al. impact force model should be seen in its favour, as it is better for the numerical solution and is supposed to better describe the contact phenomena physicality. Nevertheless, deeper analysis of the mathematical relation of the Flores et al. model reveals a problem with its application for multipoint impact. The expression for the hysteresis damping factor includes the division by the impact velocity initial value. Such division poses no problems for the impact of two bodies, as the initial velocity must be non-zero for the impact to occur. In the case of multipoint impact, where several bodies can be in contact with zero relative velocity shortly before the initiating impact occurs, this results in the division by zero. Therefore, the impact force model proposed by Flores et al. cannot be used for the modelling of multipoint impact in the system defined in the scope of this article. Consequently, the mathematical equations given subsequently utilized the impact force model proposed by Michalczyk.

Mathematical model

Although the analysed system included a maximum of six bodies (j = 1...6), the equations below were given in a general form. Such a general form yields equations of a given system for any number of bodies. From a given number of bodies, the first and last bodies require additional comment. Those two bodies, as opposed to the rest, interact only with one body. Therefore, the equation quantities with the bottom index "j" equal to 0 and m, where m is the number of bodies in the system, are not defined and assumed to be 0.

The equations use the rotation matrix B. This allows the transformation of vector coordinates expressed in the $O_j n_j t_j$ coordinate system to coordinates of the $C_j x_j y_j$ coordinate system. The angle α_j expresses rotation between those two coordinate systems. The material parameters E_j and v_j are, respectively, Young's modulus and Poisson's ratio. The values p_j are the radii of spheres used to describe the geometry of the impacting bodies in the vicinity of the contact points. The equations utilize the Coulomb-Antonow model of friction and denote the COF as μ_j. The vectors with the upper index "w" are unit vectors for a given axis. For example, $\vec{n}_1^{\,w}$ is the unit vector of the axis n_1. The remaining quantities used by the equations are either defined by them, explained above, or can be found in **Fig. 1**.

$$M_j \dot{x}_j = F_{j-1}^x \Gamma_{j-1} - T_{j-1}^x \Gamma_{j-1} \Lambda_{j-1} sgn\left(\dot{\eta}_{j-1}\right) + F_j^x \Gamma_j - T_j^x \Gamma_j \Lambda_j sgn\left(\dot{\eta}_j\right) \tag{3}$$

$$M_j \dot{y}_j = F_{j-1}^y \Gamma_{j-1} - T_{j-1}^y \Gamma_{j-1} \Lambda_{j-1} sgn\left(\dot{\eta}_{j-1}\right) + F_j^y \Gamma_j - T_j^y \Gamma_j \Lambda_j sgn\left(\dot{\eta}_j\right) \tag{4}$$

$$J_j \dot{\varphi}_j = r_{O_{j-1}/C_j}^y F_{j-1}^x - r_{O_{j-1}/C_j}^x F_{j-1}^y + r_{O_j/C_j}^y F_j^x - r_{O_j/C_j}^x F_j^y \tag{5}$$

$$\Gamma_j = \begin{cases} 1 & for \quad \xi_j > 0 \\ 0 & for \quad \xi_j \le 0 \end{cases} \tag{6}$$

$$\Lambda_j = \begin{cases} 1 & for \quad \dot{\eta}_j \ne 0 \\ 0 & for \quad \dot{\eta}_j = 0 \end{cases} \tag{7}$$

$$\vec{S}_j = \left\{ k_j^H \xi_j^{\frac{3}{2}} \left(1 - \frac{1 - R_j^2}{2} \left[1 - sgn\left(\dot{\xi}_j\right) \right] \right) \right\} \vec{n}_j^{\,w} \tag{8}$$

$$\vec{T}_j = \left\{ \mu_j S_j \right\} \vec{t}_j^{\,w} \tag{9}$$

$$\vec{F}_j = \boldsymbol{B_j}\left(\vec{S}_j + \vec{T}_j\right) \tag{10}$$

$$\boldsymbol{B}_j = \begin{bmatrix} cos(\alpha_i) & sin(\alpha_i) \\ -sin(\alpha_i) & cos(\alpha_i) \end{bmatrix} \tag{11}$$

$$\xi_j = \vec{n}_j^w \cdot \left(\vec{r}_j + \vec{r}_{O_j} - \vec{r}_{j+1} - \vec{r}_{O_{j+1}}\right) \tag{12}$$

$$\eta_j = \vec{t}_j^w \cdot \left(\vec{r}_j + \vec{r}_{O_j} - \vec{r}_{j+1} - \vec{r}_{O_{j+1}}\right) \tag{13}$$

$$\vec{r}_j = x_j \vec{x}_j^w + y_j \vec{y}_j^w \tag{14}$$

$$\vec{r}_{O_j} = \left(-\varphi_j r_{O_j/C_j}^y\right)\vec{x}_j^w - \left(\varphi_j r_{O_j/C_j}^x\right)\vec{y}_j^w \tag{15}$$

$$k_j^H = \frac{4}{3}\frac{E_j E_{j+1}}{E_j\left(1-\nu_j^2\right) + E_{j+1}\left(1-\nu_{j+1}^2\right)}\sqrt{\frac{p_j p_{j+1}}{p_j + p_{j+1}}} \tag{16}$$

Simulated cases

The simulation was based on multiple parameters; it allowed various analyses to be conducted, which could generate vast amounts of data, which difficult to comprehend and transform into knowledge. To avoid such a situation, several cases were defined. Each case focused on another aspect and simplified the simulated model. The cases were described as follows:

Case 1

All analysed impacts were central, collinear, and the initial angular velocity of the body initiating impact was equal to 0. The number of bodies included in the analysis varied from 3 to 6. This case was intended to study the influence of the number of bodies participating in the multipoint impact on the initiating impact force and to check how the simulation results correspond to the measurement data presented in **[L. 25]**. Ideally elastic impacts were simulated.

Case 2

This case studied how the changing eccentricity and the COF value influence the sliding of the bodies during impact. To quantify eccentricity, the parameter β was defined by Eq. (17). If the impact starts with sliding, there are several possible scenarios which can occur until it terminates; the sliding can continue through the duration of the impact until it terminates, the sliding can stop and stay in that state or reverse its direction. This case analysed which scenario occurs depending on the value of the COF and the value of eccentricity expressed by the parameter β.

$$\beta = \frac{\left(M_1^{-1} + M_2^{-1}\right)^{-1} r_{O_{j-1}/C_j}^y r_{O_{j-1}/C_j}^x}{J_1} \tag{17}$$

Case 3

The third case investigated various angles at which the initiating impact can occur and different values of the COR. The initial position of Body 1 was varied in such a way that the angle between the n_1 axis of the initiating impact local coordinate system and the x axis of the global coordinate system changed from 0 to 75 degrees. The influence of these changes on the impact force was then investigated while the rest of the multipoint impacts were kept collinear. This case also showed how changing the amount of energy dissipation expressed by the COR influences the impact forces.

The contact stiffness parameters are dependent on the material's Young's modulus, Poisson's ratio, and the curvature of the contacting surfaces in the vicinity of the contact point. Although the various contact stiffness for each of the multipoint impacts can change the behaviour of the system, its investigation was outside the scope of this article. Therefore, the Young's modulus was set for

each body to be equal $E = 2.05 \cdot 10^{11}$ Pa together with the Poisson's ratio $\upsilon = 0.3$ **[L. 29]**, and it was assumed that the curvature of each contacting body in the vicinity of the contact point can be described by the sphere of the radius equal to 0.05 m.

RESULTS AND DISCUSSION

The equations given in the previous section were implemented in the Python programming language. For this purpose, the open source libraries of Numpy, Scipy, Matplotlib, and Math were used. Those libraries offer various tools, of which the efficient implementation of array operations and the algorithms for the solution of the ODEs (Ordinary Differential Equations) seem the most important in the context of this article. To solve the ODEs, a variable coefficient algorithm named VODE **[L. 39]** was used.

The implementation consisted of several hundreds of code lines. Although it seems not many, it was still prone to errors, especially in the functions implementing ODEs. To ensure that all errors were eliminated, the simulation was equipped with two checking mechanisms. The first mechanism calculated the kinetic energy of all bodies and the energy dissipated due to the friction and restitution; next, it compared the result with the initial kinetic energy of the body initializing impact. Both quantities should be equal. If this condition was not satisfied with a given error threshold, the simulation raised an error. The second mechanism checked the conservation of the linear and angular momentum. If, in any time step of the simulation, the momentum was not conserved with a given error threshold, an error was raised.

Results of case 1

The impact forces calculated by the simulation for this case are presented in **Fig. 3**. It can be easily observed (for example, by drawing lines parallel to the force axis and counting the points in which the plot curves are crossed by it) that, at any time instant, the impact takes place at a maximum of 3 points. Therefore, there is no difference in the initiating impact force between systems with 4, 5, and 6 bodies. Moreover, a closer look at **Fig. 3** indicates that there is only a short overlap between the first and third impact. This fact suggests that, if the impact force of the initiating impact is the goal of the simulation, including only 3 bodies in it will be a good approximation. This was confirmed by the data given in **Table 1**. It showed no difference (to the error of rounding) in the value of the maximum impact force for the initiating impact and very small differences in the duration time and resulting velocity between simulations performed with 3, 4, 5, and 6 bodies. The data obtained also corresponds well with the experimental results presented by **[L. 25]**.

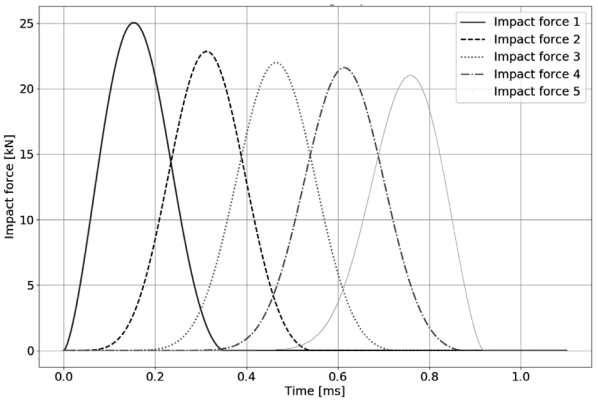

Fig. 3. The impact forces for the system of six bodies obtained for the configuration defined in Case 1

Rys. 3. Siły zderzenia dla układu sześciu ciał otrzymane dla zderzenia zdefiniowanego w przypadku 1

Table 1. The values of the maximum impact force, the duration time and the velocity obtained for Body 1 for the simulation with 3, 4, 5, and 6 bodies

Tabela 1. Wartości maksymalnych sił zderzenia, jego czasu trwania oraz prędkości ciała 1 dla przypadków symulacji uwzględniających 3, 4, 5 oraz 6 ciał biorących udział w zderzeniu

Number of bodies	Value of maximum impact force for the first impact [kN]	Duration time of the first impact [ms]	Velocity of the first body after impact [m/s]
3	25.05	0.345	0.07
4	25.05	0.35	0.071
5	25.05	0.35	0.071
6	25.05	0.35	0.071

Results of case 2

The results of the simulations conducted for this case are presented in **Fig. 4**. This figure summarised possible developments of the sliding process as a function of the COF and the parameter β, which expressed the level of the impact eccentricity.

As evident from **Fig. 4a**, the sliding process of the impacting bodies could be divided into 3 main regions. There was a fundamental difference in the sliding behaviour in them and they were separated approximately by two lines. Those lines were kept the same for plots in **Figs. 4b** and **4c** to clearly show the differences. In the region marked by triangles, the sliding velocity dropped to 0 and then reversed its direction. The region marked by pluses represented parameter values for which the sliding velocity continuously increased its value, resulting in continuous slip during the impact.

The last region, marked with circles, showed areas where the sliding velocity dropped to 0 and then stuck. To show the results in more detail, an additional

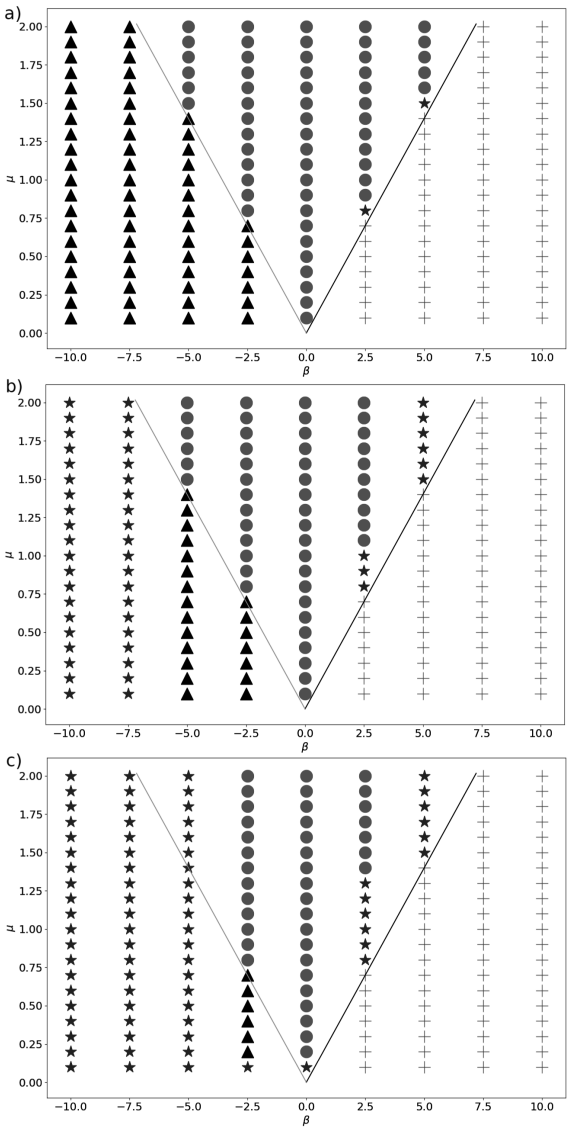

Fig. 4. Possible developments of the sliding process as a function of the COF and parameter β; a) for Φ_0 = 0.1, b) for Φ_0 = 0.5, c) for Φ_0 = 1. Symbols used for the sliding regions: triangle (slip-reverse slip), circle (slip-stick), plus (increasing sliding velocity – continuous slip), star (decreasing sliding velocity, 0 not reached)

Rys. 4. Możliwe scenariusze rozwoju poślizgu jako funkcja współczynnika tarcia i parametru β; a) dla Φ_0 = 0.1, b) dla Φ_0 = 0,5, c) dla Φ_0 = 1. Symbole użyte do oznaczenia poszczególnych regionów: trójkąt (poślizg–zmiana kierunku poślizgu), koło (poślizg–zatrzymanie poślizgu), plus (wzrastająca prędkość poślizgu – ciągły poślizg), gwiazdka (malejąca prędkość poślizgu – ciągły poślizg)

minor region was introduced. It was marked by a star and represented situations where the sliding velocity was decreasing but did not reach 0 value during the impact time. Therefore, such behaviour could occur in the region of the reversed slip (triangles) or the stick (circles) and was dependent on the value of the COF and the parameter Φ_0, which expressed the relation between components of the initiating body velocity and was given by Eq. 18. **Figure 4** presents results for three different values of the parameter Φ_0 = (0.1, 0.5, 1). It is evident that, although for greater values of the parameter Φ_0 the friction force was not able to bring initial sliding to 0 (situation marked with a star), the general behaviour of the region was kept. This means that, in regions of slip-reverse slip and slip-stick, the appropriate behaviour (reversing sliding direction or sticking) is to always be expected when sliding velocity drops to 0.

Figure 4a demonstrates that the sliding regions in the investigated space were almost symmetrical. The asymmetry grows with the increasing value of the parameter Φ_0, as presented in **Figs. 4b** and **4c**. Such behaviour was justified by the different body configurations. On the right hand side of the plots shown in **Fig. 4**, the bodies had a tendency to increase the sliding velocity, which resulted in the slower transformation into the slip-stick region and meant that the results were not affected by the parameter Φ_0. This was a logical result as the value at which sliding velocity starts increasing does not matter.

The COF and the configuration of other bodies taking part in the multipoint impact also influenced the sliding process of the initiating impact, but this influence was not deeply investigated and will be the subject of further research. In the presented results, the sliding process in the initiating impact was mainly influenced by other bodies taking part in the multipoint impact through the normal impact force, which was directly linked to the friction force by the Coulomb-Antonow friction law.

$$\Phi_0 = \frac{\dot{y}_1^0}{\dot{x}_1^0} \tag{18}$$

where $\dot{y}_1^0$, $\dot{x}_1^0$ are components of the initial velocity of body 1, which initiates impact.

Results of case 3

Figure 5 shows the impact forces in the system with the COR equal to 0.8 for all impacts and the angle α describing the initiating impact direction equal to 30 degrees. Those forces revealed several differences when compared with the forces in **Fig. 3**. The dissipation of the kinetic energy introduced by the COR caused the subsequent impacts to be less intensive, which resulted in a lower value of the maximum impact force. In other words, the maximum impact force of subsequent impacts declined essentially faster after a decrease in the COR. **Figure 5** also shows weak spots of the selected impact force model. The discontinuity of the impact force caused a noticeable reduction of the integration time, resulting in drastically higher calculation time. Moreover, the duration of the impacts increased. For the COR equal to 0.8, there was already a clear overlap between the first and fourth impact forces. Additionally,

the duration of the fourth impact was longer than the duration of the fifth impact, which contradicted common sense.

The changes in the initiating impact force for different values of the COR and angle α are presented in **Fig. 6**. Because the impact force model does not include the energy dissipation in the compression phase of the impact, the value of the maximum impact force shown in **Fig. 6** depended only on the angle α. The influence of this parameter on the maximum impact force value was significant. With the increasing value of the angle α, the maximum impact force value dropped dramatically. The analysis of this result led to the conclusion that the increasing value of the angle α limited the influence of other bodies in the chain on the initiating impact, causing it to be more a two-body event. The effect of the changing value of the COR could be clearly seen at the time point which separates the compression and restitution phase of the impact. With the increasing value of the COR, the relative drop of the impact force was bigger. Additionally, the duration of the impact increased slightly.

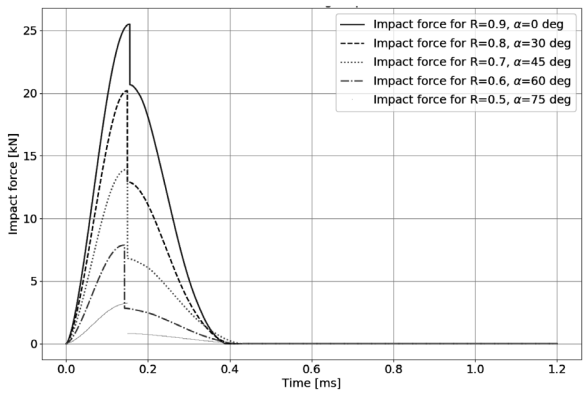

Fig. 5. Impact forces for COR equal to 0.8 for all impacts and angle α equal to 30 degrees

Rys. 5. Siły zderzenia dla współczynnika restytucji równego 0,8 dla wszystkich zderzeń i kąta α wynoszącego 30 stopni

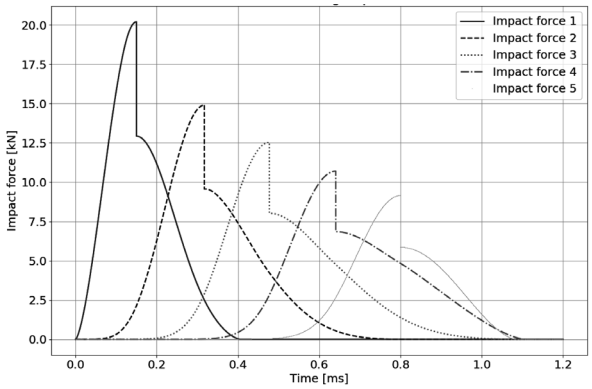

Fig. 6. The first impact force for various values of the parameters R and α

Rys. 6. Siły zderzenia inicjującego dla różnych wartości parametrów R oraz α

SUMMARY

This article presented a mathematical model of the multipoint impact in a planar multibody system. The developed model included the friction phenomenon and the kinetic energy dissipation expressed by the COR and allowed various simulation investigations to be conducted. Those investigations were divided into three cases. The conclusions resulting from these investigations can be summarized briefly, as in the following points:

- Approximately 3 bodies take part in the multipoint impact at a given time point. This corresponds well with the experimental data.
- The sliding process during the impact can be divided into three main regions: continuous slip with increasing sliding velocity, slip-reversal slip, and slip-stick. The development of the sliding process depends on the COF and the impact eccentricity level expressed by the defined parameter β.
- The sliding process is also impacted in a minor way by the initial sliding velocity. If it has an excessively high value to be stopped during the impact, in the range of stick-reversal slip and stick-slip, continuous sliding with decreasing sliding velocity is to be expected.
- The direction of the initiating impact has a significant influence on the maximum impact force. With the increase of the incidence angle, the maximum impact force dropped dramatically.

The simulation investigations also showed weak spots of the implemented impact force model. The discontinuity of the impact force causes numerical problems with the solution and increases the computational time. Additionally, the duration time of the restitution phase increases with the decreasing value of the COR. This led to a situation contradicting common sense, when the last impact duration was shorter than the preceding one. Therefore, this impact force model requires improvements for better applicability in multipoint impact, which will be the subject of further research.

Acknowledgement: The author acknowledge the financial support of AGH University of Science and Technology, project No. 16.16.130.942.

REFERENCES

1. Kakizaki T., Deck J.F., and Dubowsky S.: Modeling the Spatial Dynamics of Robotic Manipulators with Flexible Links and Joint Clearances'. J. Mech. Des., vol. 115, no. 4, pp. 839–847, Dec. 1993, doi: 10.1115/1.2919277.
2. Warzecha M., Michalczyk J.: Calculation of maximal collision force in kinematic chains based on collision force impulse'. J. Theor. Appl. Mech., vol. 58, no. 2, 2020, pp. 339–349, doi: 10.15632/jtam-pl/116580.
3. Zhang D.-G., Angeles J.: Impact dynamics of flexible-joint robots. Comput. Struct., vol. 83, no. 1, pp. 25–33, 2005.
4. Stronge W. J.: Rigid body collisions with friction. Proc. R. Soc. Lond. Ser. Math. Phys. Sci., vol. 431, no. 1881, pp. 169–181, Oct. 1990, doi: 10.1098/rspa.1990.0125.
5. Stronge W. J.: Friction in collisions: Resolution of a paradox. J. Appl. Phys., vol. 69, no. 2, 1991, pp. 610–612, doi: 10.1063/1.348922.
6. Wang Y., Mason M.T.: Two-Dimensional Rigid-Body Collisions With Friction. J. Appl. Mech., vol. 59, no. 3, 1992, pp. 635–642, doi: 10.1115/1.2893771.
7. Stronge W.J.: Smooth dynamics of oblique impact with friction. Int. J. Impact Eng., vol. 51, 2013, pp. 36–49, doi: 10.1016/j.ijimpeng.2012.08.001.
8. Glocker Ch., Pfeiffer F.: Multiple impacts with friction in rigid multibody systems. Nonlinear Dyn., vol. 7, no. 4, 1995, pp. 471–497.
9. Pereira M.S., Nikravesh P.: Impact dynamics of multibody systems with frictional contact using joint coordinates and canonical equations of motion. Nonlinear Dyn., vol. 9, no. 1–2, 1996, pp. 53–71.
10. Adams G.G.: Imperfectly constrained planer impacts – a coefficient-of-restitution model. Int. J. Impact Eng., vol. 19, no. 8, 1997, pp. 693–701.
11. Ceanga V., Hurmuzlu Y.: A New Look at an Old Problem: Newton's Cradle. J. Appl. Mech., vol. 68, no. 4, 2000, pp. 575–583.
12. Warzecha M.: A comparative analysis of sequential and simultaneous approach in collision modeling. Model. Eng., vol. 35, no. 66, 2018, pp. 81–86.
13. Stronge W.J.: Mechanics of Impact for Compliant Multi-Body Systems. in IUTAM Symposium on Unilateral Multibody Contacts, vol. 72, F. Pfeiffer and Ch. Glocker, Eds. Dordrecht: Springer Netherlands, 1999, pp. 137––144.
14. Machado M., Moreira P., Flores P., and Lankarani H. M.: Compliant contact force models in multibody dynamics: Evolution of the Hertz contact theory. Mech. Mach. Theory, vol. 53, 2012, pp. 99–121.
15. Khulief Y.A.: Modeling of impact in multibody systems: an overview. J. Comput. Nonlinear Dyn., vol. 8, 2013, pp. 021012-1–15.
16. Skrinjar L., Slavič J., Boltežar M.: A review of continuous contact-force models in multibody dynamics. Int. J. Mech. Sci., vol. 145, 2018, pp. 171–187, doi: 10.1016/j.ijmecsci.2018.07.010.
17. Thornton C.: Coefficient of restitution for collinear collisions of elastic-perfectly plastic spheres. J. Appl. Mech., vol. 64, no. 2, 1997, pp. 383–386.
18. Mesarovic S. Dj., FleckN. A.: Frictionless indentation of dissimilar elastic-plastic spheres. Int. J. Solids Struct., vol. 37, no. 46–47, 2000, pp. 7071–91.
19. Půst L., Peterka F.: Impact Oscillator with Hertz's Model of Contact. Mechanica, vol. 38, no. 1, 2003, pp. 99–116, doi: 10.1023/A: 1022075519038.
20. Du Y., Wang S.: Energy dissipation in normal elastoplastic impact between two spheres. J. Appl. Mech., vol. 76, no. 6, 2009, p. 061010.
21. Big-Alabo A.: Rigid body motions and local compliance response during impact of two deformable spheres. Mech. Eng. Res., vol. 8, no. 1, 2018, pp. 1–15.
22. Stronge W. J., James R., Ravani B.: Oblique impact with friction and tangential compliance. Philos. Trans. R. Soc. Lond. Ser. Math. Phys. Eng. Sci., vol. 359, no. 1789, pp. 2447–2465, Dec. 2001, doi: 10.1098/rsta.2001.0903.
23. Cross R.: Grip-slip behavior of a bouncing ball. Am. J. Phys., vol. 70, no. 11, 2002, pp. 1093–102 .
24. Stronge W. J.: Chain Reaction From Impact on Coaxial Multibody Systems. J. Appl. Mech., vol. 67, no. 3, 2000, pp. 632–635, doi: 10.1115/1.1309541.
25. Singh R., Shukla A., Zervas H.: Explosively generated pulse propagation through particles containing natural cracks. Mech. Mater., vol. 23, no. 4, 1996, pp. 255–270, doi: 10.1016/0167-6636(96)00026-9.
26. Lankarani H.M., Nikravesh P.: Continuous Contact Force Models for Impact Analysis in Multibody Systems. Nonlinear Dyn., vol. 5, no. 2, 1994, pp. 193–207.
27. Hertz H.: Ueber die Berührung fester elastischer Körper. J. Für Reine Angew. Math. Crelles J., vol. 1882, no. 92, 1982, pp. 156–171, doi: 10.1515/crll.1882.92.156.

28. Yang D.C.H., Sun Z.S.: A Rotary Model for Spur Gear Dynamics. J. Mech. Transm. Autom. Des., vol. 107, no. 4, 1985, pp. 529–535, doi: 10.1115/1.3260759.
29. Goldsmith W.: Impact: the theory and physical behaviour of colliding solids. London: Edward Arnold Ltd., 1960.
30. Brake M.R.: An analytical elastic-perfectly plastic contact model. Int. J. Solids Struct., vol. 49, no. 22, 2012, pp. 3129–3141, doi: 10.1016/j.ijsolstr.2012.06.013.
31. Brake M.R.: An analytical elastic plastic contact model with strain hardeningand frictional effects for normal and oblique impacts. Int. J. Solids Struct., vol. 62, 2015, pp. 104–23.
32. Michalczyk J.: Phenomenon of Force Impulse Restitution in Collision Modelling. J. Theor. Appl. Mech., vol. 46, no. 4, 2008, pp. 897–908.
33. Hunt K.H., Crossley F.R.E.: Coefficient of Restitution Interpreted as Damping in Vibroimpact. J. Appl. Mech., vol. 42, no. 2, 1975, pp. 440–445, doi: 10.1115/1.3423596.
34. Herbert R.G., McWhannell D.C.: Shape and Frequency Composition of Pulses From an Impact Pair. J. Eng. Ind., vol. 99, no. 3, 1977, pp. 513–518, doi: 10.1115/1.3439270.
35. Lankarani H.M., Nikravesh P.E.: A Contact Force Model With Hysteresis Damping for Impact Analysis of Multibody Systems. J. Mech. Des., vol. 112, no. 3, 1990, pp. 369–376, doi: 10.1115/1.2912617.
36. Gonthier Y., McPhee J., Lange C., Piedbœuf J.-C.: A Regularized Contact Model with Asymmetric Damping and Dwell-Time Dependent Friction. Multibody Syst. Dyn., vol. 11, no. 3, 2004, pp. 209–233, doi: 10.1023/B:MUBO.0000029392.21648.bc.
37. Flores P., Machado M., Silva M. T., Martins J. M.: On the continuous contact force models for soft materials in multibody dynamics. Multibody Syst. Dyn., vol. 25, no. 3, 2011, pp. 357–375, doi: 10.1007/s11044-010-9237-4.
38. Yu J., Chu J., LiY., and GuanL.: An improved compliant contact force model using a piecewise function for impact analysis in multibody dynamics. Proc. Inst. Mech. Eng. Part K J. Multi-Body Dyn., 2020, p. 146441931990087, doi: 10.1177/1464419319900874.
39. Brown P.N., Byrne G.D., Hindmarsh A. C.: VODE: a variable-coefficient ODE solver. J. Sci. Stat. Comput., vol. 10, 1989, pp. 1038–1051.